

PERFORMANCE MEASUREMENT OF MEDICAL IMAGING SYSTEMS BASED ON MUTUAL INFORMATION METRIC

*Eri Matsuyama*¹, *Du-Yih Tsai*¹, *Yongbum Lee*¹, and *Katsuyuki Kojima*²

¹Department of Radiological Technology, Graduate School of Health Sciences, Niigata University, 2-746, Asahimachi-dori, Chuo-ku, Niigata, 951-8518, Japan, tsai@clg.niigata-u.ac.jp

²Department of Information Networks, Faculty of Administration and Informatics, University of Hamamatsu, 1230, Miyakodacho, Kita-ku, Hamamatsu, 431-2102, Japan, kojima@hamamatsu-u.ac.jp

Abstract – Information on physical image quality of medical images is important for imaging system assessment in order to promote and stimulate the development of state-of-the-art imaging systems. In this paper, we present a method for measuring physical performance of medical imaging systems. In this method, mutual information (MI) which is a concept from information theory was used to measure combined properties of image noise and resolution of an imaging system. In our study, the MI was used as a measure to express the amount of information that an output image contains about an input object. The more the MI value provides, the better the image quality is. To validate the proposed method, computer simulations were first performed to investigate the effects of noise and resolution degradation on the MI. Then experiments were conducted to measure the physical performance of an imaging plate which was used as an image detector. Our simulation and experimental results confirmed that the combined effect of deteriorated blur and noise on the images can be measured and analyzed using the MI metric. The results demonstrate the potential usefulness of the proposed method for measuring physical quality of medical imaging systems.

Keywords: image quality, medical imaging, mutual information

1. INTRODUCTION

An important criterion for accepting any type of medical imaging system is the quality of the images produced by the imaging systems. The most fundamental quality-related factors in medical imaging systems are contrast, spatial resolution and noise. It is customary to describe contrast by the characteristic curve of the system, spatial resolution by the modulation transfer function (MTF), and noise by the noise power spectrum (NPS, also referred to as the Wiener spectrum) [1, 2]. One of the current dilemmas in digital radiography is the extent to which these parameters such as, resolution and noise affect physical or clinical image quality. An imaging system may only be superior in one metric while being inferior to another in the other metric.

In this study we present an information-entropy-based approach for measuring overall image quality (including image noise and spatial resolution in this study) in medical

imaging systems. The approach uses mutual information (MI) in information theory [3, 4] as an image quality criterion. Differing from the MTF and NPS measures, this information-entropy-based metric is described in the spatial domain. The concept of MI has been applied in medical imaging processing, in particular for image registration tasks and computer-assisted detection schemes [5-7]. However, the application of MI as an overall quality metric has been rather limited so far [8, 9]. The primary motivation behind this study was to use the MI to express the amount of information that an output image contains about an input object (subject). The basic idea is that when the amount of the uncertainty associated with an object before and after imaging is reduced, the difference of the uncertainty is equal to the value of MI. The more the MI value provides, the better the image quality is. Therefore, we can quantitatively evaluate the overall quality of an image by measuring the MI. The present work is an extension of the aforementioned studies [8, 9]. The focus of this paper is to investigate and characterize the combined effect of noise and blur on the images obtained from medical imaging systems using the proposed metric. The advantages of our proposed method are: (1) simplicity of computation, (2) simplicity of experimentation, and (3) combined assessment of image noise and resolution.

In the present study, simulation studies were first carried out to investigate the relationship between noise and the MI, as well as that between spatial resolution and the MI. To validate the proposed method, two experiments were then performed. The first experiment was conducted for verifying the effect of noise on the MI value. The second experiment was carried out for analyzing the effect of image blurring on the MI value. Furthermore, in order to compare the proposed method with the conventionally used metrics, the presampling MTF and NPS were also calculated and discussed. In addition, two imaging plates, a high resolution type detector and a standard resolution type detector, for computed radiography were used for verification of the potential usefulness of the MI metric. The verification was made by showing two real images with detailed discussion. Results show that the proposed method is simple to implement, and has potential usefulness for evaluation of overall image quality.

2. MUTUAL INFORMATION

Mutual information (MI) is a basic concept in information theory. It has been introduced for the registration of multimodality medical images. The definition of the term has been presented in various ways in the literature [10]. We will briefly describe the MI used for measurement of image quality.

Given events s_1, \dots, s_n occurring with probabilities p_1, p_2, \dots, p_n , the Shannon entropy H is defined as

$$H(p_1, p_2, \dots, p_n) = -\sum_{i=1}^n p_i \log_2 p_i. \quad (1)$$

Considering x and y as two random variables corresponding to an input variable and an output variable, the entropy for the input and that for the output are denoted as $H(x)$ and $H(y)$, respectively. For this case, the MI can be defined as

$$\begin{aligned} MI(x; y) &= H(x) - H_y(x) = H(y) - H_x(y) \\ &= H(x) + H(y) - H(x, y), \end{aligned} \quad (2)$$

where $H(x, y)$ is the joint entropy, and $H_x(y)$ and $H_y(x)$ are conditional entropies. The relationship among these entropies is shown in Fig. 1.

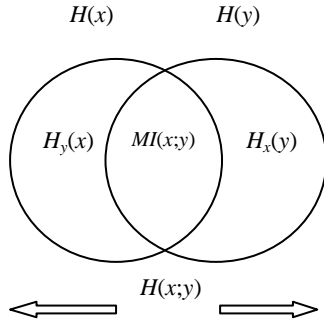


Fig. 1. Relationship among $H(x)$, $H(y)$, $H(x, y)$, $H_x(y)$, $H_y(x)$, and $MI(x; y)$.

Consider an experiment in which every input has a unique output belonging to one of the various output categories. In this study, for simplicity, the inputs may be considered to be a set of subjects (for example, a test sample object with steps of various thickness, while the outputs may be their corresponding images varying in optical density or gray level. A method of occurrence-frequency-based computation is employed in the present study for calculating the entropies of input, output, and their joint entropies [11]. With this orderly system, the amount of MI is easily computed. The MI conveys the amount of information that output y has about input x .

3. METHODS AND MATERIALS

3.1. Computer Simulation

A simulation was designed and its framework is as follows. In mathematical terms, a simulation image $g(x, y)$ is the convolution of a uniformly-distributed signal (an object) $f(x, y)$ and the blurring function B . If the noise $u(x, y)$ is also

taken into consideration, the resulting image may be represented by the following formula:

$$g(x, y) = \sum_{k=1}^5 \{ [k \times f(x, y)] * B + u(x, y) \times W \}, \quad (3)$$

where the symbol $*$ represents the convolution operation, B is a blurring function, and k is an integer representing the number of steps of the simulated image. In this simulation study, the input image $f(x, y)$ is a five-step wedge with a specific intensity or pixel value on each step. The term of W is a weighting coefficient used to adjust the extent of noise, and $u(x, y)$ is a zero-mean Gaussian noise with a standard deviation of 0.5.

Two simulations were performed separately. The first simulation was carried out to investigate the relationship between image noise and the MI. We employed signal-to-noise ratio (SNR) to describe the extent of noise level. The signal and noise used for SNR calculation were $k \times f(x, y) * B$ and $u(x, y) \times W$, respectively, as given in (3). As a blurring function, we used a neighborhood averaging filter with a size of $m \times m$ (m is an odd integer). The extent of blurring was adjusted by varying the filter size. The reason for choosing neighborhood averaging filter was due to its commonality and simplicity of operation. The second simulation was conducted to investigate the relationship between the blurring (spatial resolution) and the MI.

An image of a simulated step wedge is shown in Fig. 2 (a). Five regions of interests (ROIs) indicated with dotted rectangles near the boundaries of two adjacent steps were chosen for calculation of the MI. The five steps of the step-wedge image are numbered from the right side as step 1, step 2, ..., and step 5. The area at the right side without dotted rectangle is the background of the image. The corresponding pixel-value distributions measured from the ROIs are given in Fig. 2 (b). The area of each ROI used in this study was 50×200 pixels. As a result, a total of 10×10^3 data for each step was obtained. As shown in Fig. 2 (a), the number of inputs is five, and the number of outputs is the range of gray levels shown on the horizontal axis of the pixel-value distributions (see Fig. 2 (b)).

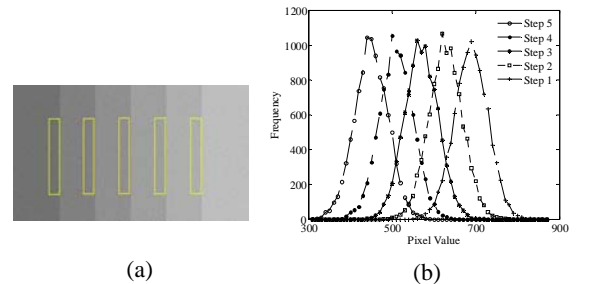


Fig. 2. (a) Computer-generated step wedge. A region of interest (ROI) shown with a dotted rectangle at each step of the step wedge was chosen for entropy computation. (b) The corresponding pixel-value distributions measured from the ROIs shown in (a).

3.2. Experiments

An acrylic step wedge 0-1-2-3-4-5 mm in thickness was used as a test sample object for experiments. The specified exposure factors were kept at 42 kV and 10 mA, and the focus-imaging distance was taken as 185 cm, but the

exposure time was varied from 0.1 sec to 0.4 sec. A tube voltage of 50 kV was also employed for comparison. An imaging plate (standard resolution type, ST, Fuji Film Japan, Inc.) was used as a detector to record x-ray intensities.

In this study, two experiments were performed. The first experiment was conducted for verifying the effect of noise properties on the measured MI value, and the second experiment was performed for analyzing the effect of resolution (blur) properties on the MI value. The experiments were carried out by varying of exposure levels and by use of various effective focal spot sizes of the X-ray tube, respectively. The latter experiment was achieved by shifting of the step wedge away from the center of the X-ray beam area toward the cathode end when imaging was performed. The effective focal spot size changes with position in the field. It becomes larger for points toward the cathode end of the field [12]. The increase in the effective focal spot size results in the degradation of resolution (blur). In addition, a high resolution type imaging plate HR for computed radiography was also used for evaluation and comparison. Moreover, two real images (the distal femur and the tarsal bone) were shown and compared for experimental validation of the advantages of the proposed method.

4. RESULTS AND DISCUSSION

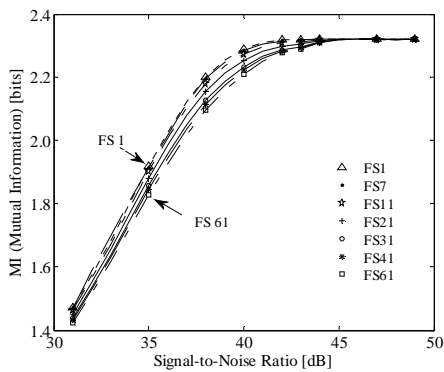


Fig. 3. Relationship between the SNR and the MI for various levels of blur at an image contrast of 20.

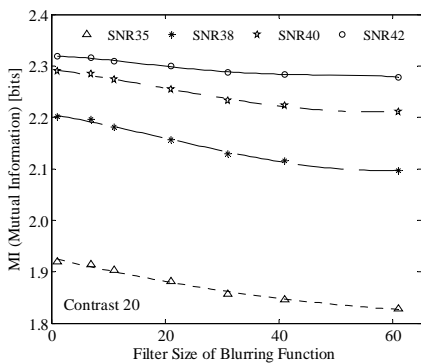


Fig. 4. Relationship between the filter size of blurring function and the MI for various levels of SNR at an image contrast of 20.

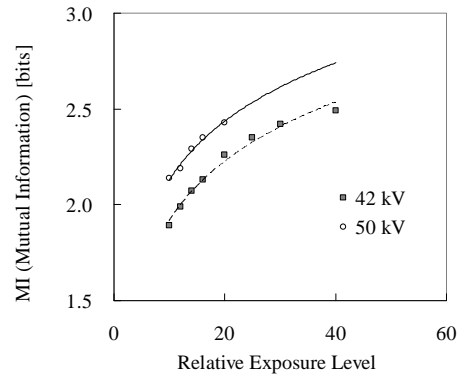


Fig. 5. Mutual information as a function of relative exposure level for tube voltages of 42 kV and 50 kV.

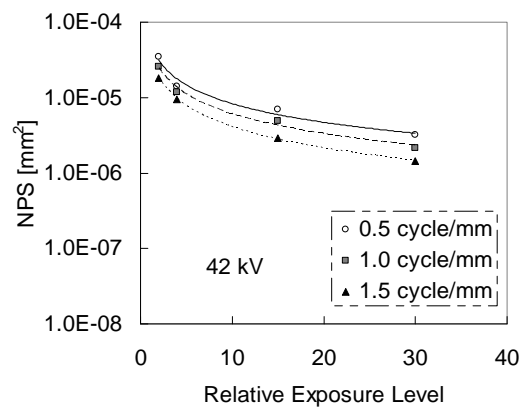


Fig. 6. Noise power spectra (NPS) as a function of relative exposure level for three spatial frequencies at 42 kV.

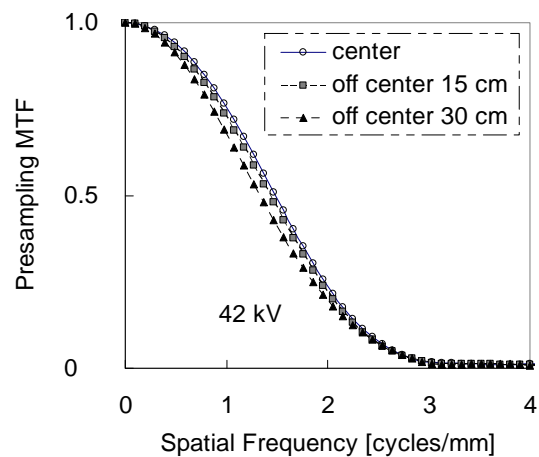


Fig. 7. Presampling MTF as a function of spatial frequency for three effective focal spot sizes, obtained by shifting of the step wedge 15 cm and 30 cm away from the center of the X-ray beam area toward the cathode end.

Simulations were performed to investigate individual effects of noise and spatial resolution on MI. Fig. 3 illustrates the MI as a function of SNR for various levels of blurring at image contrast of 20. The results indicate that

MI value increases with the increase of SNR (decrease in noise level). Fig. 4 shows the MI as a function of filter size of blurring function for various levels of SNR at image contrast of 20. The results indicate that MI value decreases when filter size of the blurring function increases (degradation of resolution). It was noted that the decline of the MI value is relatively small. It means that the effect of the level of blur on the MI is not so obvious in comparison to noise.

Fig. 5 illustrates the MI value as a function of the relative exposure level for tube voltages of 42 kV and 50 kV. The result shows that the MI value increases with the increase in the exposure level. The increase of the MI value is considered to be mainly due to the decrease of noise. Fig. 6 illustrates the NPS of the imaging system used in this study as a function of the relative exposure level at 42 kV for spatial frequencies of 0.5, 1.0, and 1.5 cycles/mm. The figure indicates that the NPS decreases with increasing exposure levels.

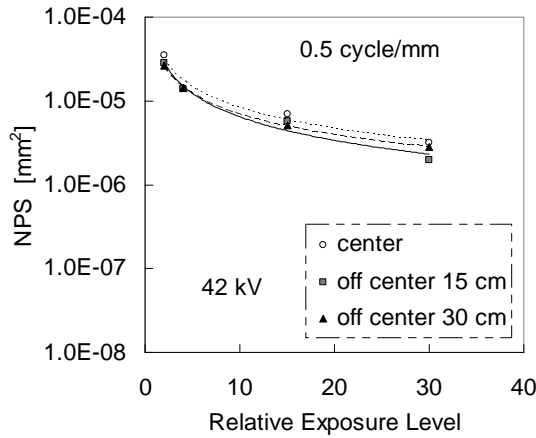


Fig. 8. Noise power spectra (NPS) as a function of relative exposure level for three effective focal spot sizes for 42 kV at the spatial frequency of 0.5 cycle/mm.

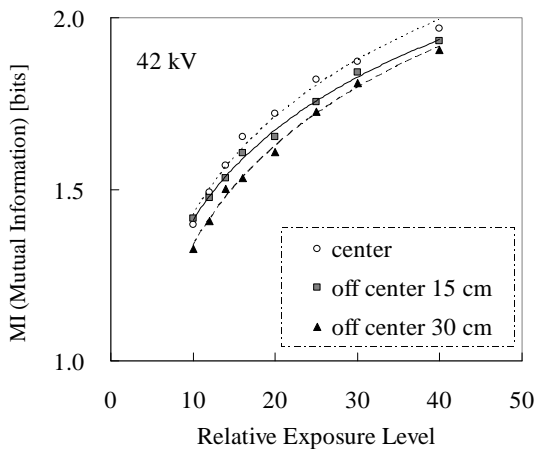


Fig. 9. Mutual information as a function of relative exposure level for three different exposure positions of the step wedge at 42 kV.

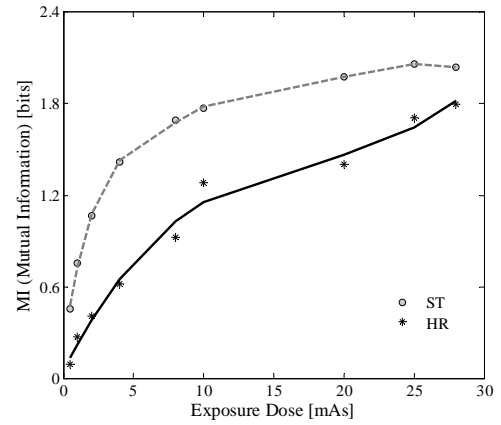


Fig. 10. Mutual information as a function of relative exposure level for ST and HR imaging plates.

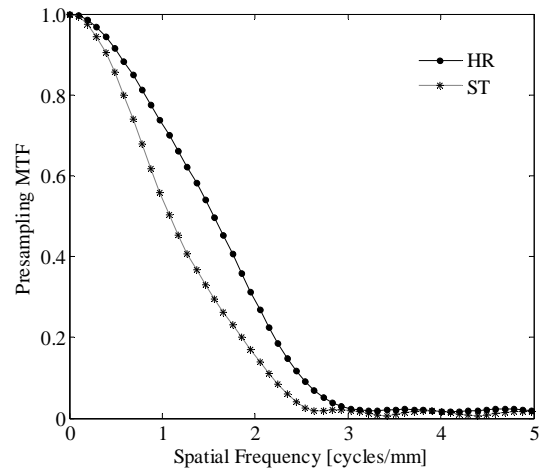


Fig. 11. Presampling MTF as a function of spatial frequency obtained with the ST and HR imaging plates.

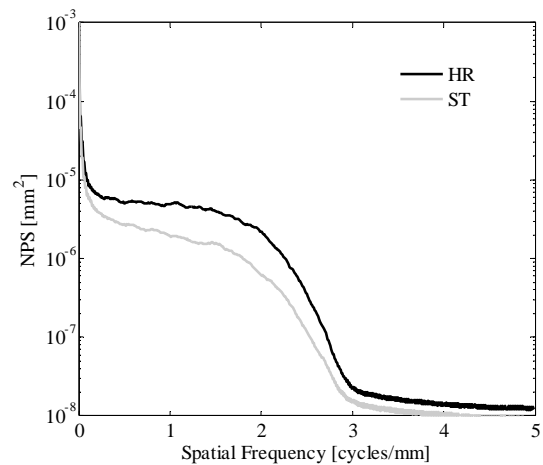


Fig. 12. NPS as a function of spatial frequency obtained with the ST (standard resolution) and HR (high resolution) imaging plates.

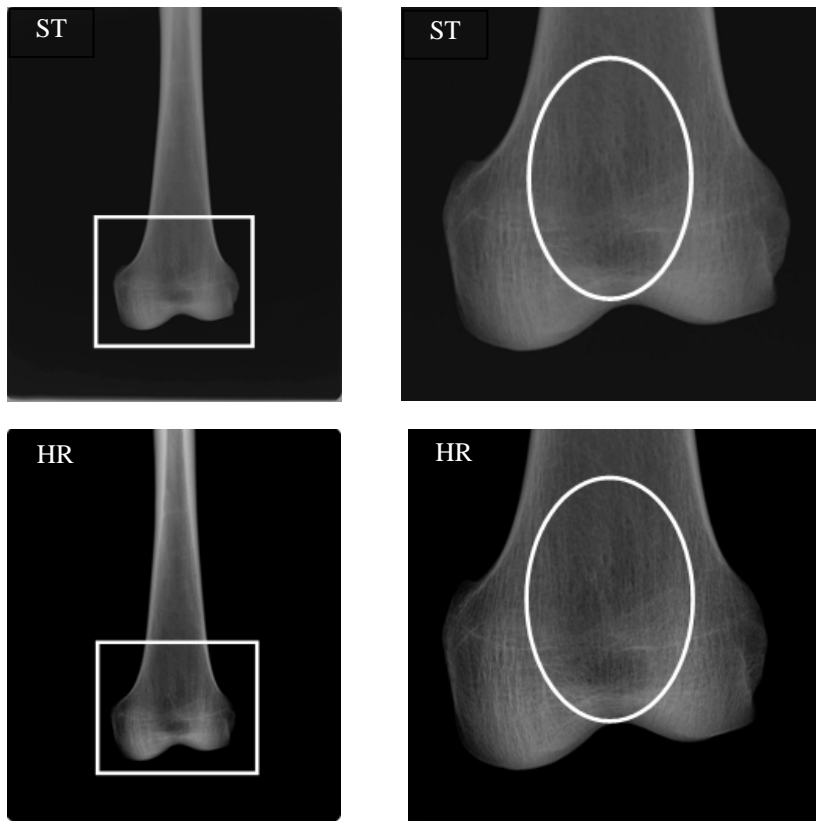


Fig. 13. Real images of the distal femur acquired with ST and HR image plates.

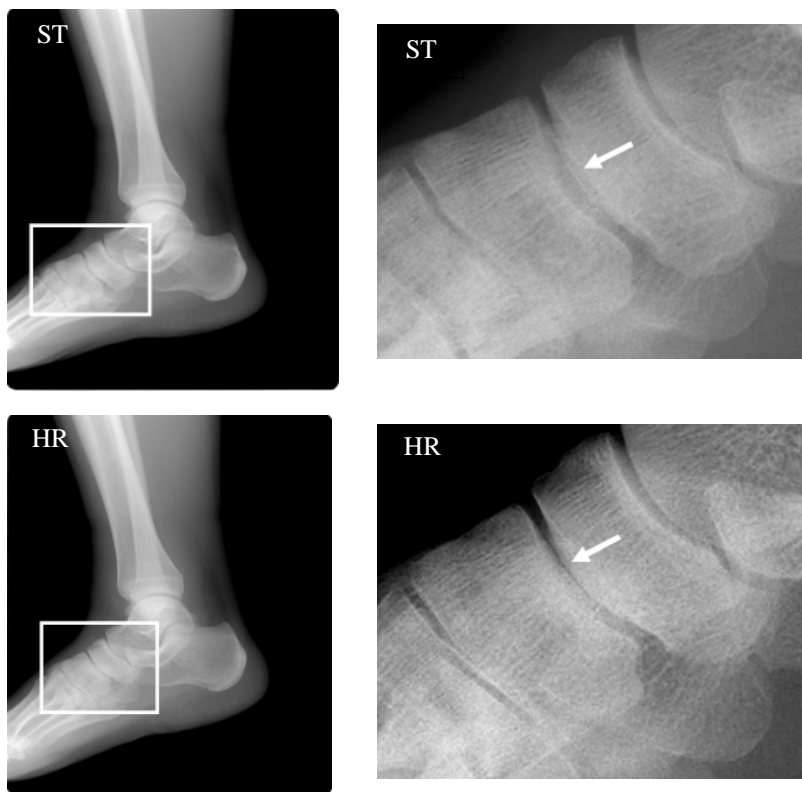


Fig. 14. Real images of the tarsal bone acquired with ST and HR image plates.

Fig. 7 shows the presampling MTF as a function of spatial frequency for three effective focal spot sizes, obtained by shifting of the step wedge 15 cm and 30 cm away from the center of the X-ray beam area toward the cathode end. The MTF was measured with an angled-edge method. Theoretically, the amount of geometric blurring increases when the size of effective focal spot increases. As shown in Fig.7, the MTF was degraded with the increase of the effective focal spot size. Fig. 8 provides the one-dimensional NPS as a function of relative exposure for the three effective focal spot sizes at spatial frequency of 0.5 cycle/mm. The difference of NPSs is moderately small. Fig. 9 is a plot of the MI values for the three effective focal spot sizes. The measured results show that the MI value becomes lower when the off-center distance is greater. In other words, the MI value decreases when the effective focal spot size increases. This means that the MI value decreases when blur is deteriorated. It is noted that the decrease of the MI is mainly due to the image blurring resulting from the increase of the effective focal spot size. Therefore, the MI is also closely correlated with the resolution (blur) of imaging systems.

Fig. 10 shows the relation between the exposure dose and the MI for the images obtained with ST and HR imaging plates. The results illustrate that the MI increases with the increase of exposure dose. The rise of MI is considered due to the decrease of noise resulting from the increase of radiation dose. As shown in the figure, the MI value for the ST plate is higher than that for the HR plate at the same exposure dose. This can be explained by the fact that combined effects of the blur and noise lead to a higher MI value for the ST plate. Fig. 11 shows the presampled MTFs of the ST and HR imaging plates. The MTF of HR imaging plate is higher than that of ST imaging plate. This means that the spatial resolution (blur) of HR plate is higher than that of ST plate. Fig. 12 illustrates the NPS of the ST and HR imaging plates used in this study. The results show that the NPS of the HR imaging plate is higher than that of the ST plate. This means that ST imaging plate has better noise properties.

In Figs. 13 and 14, we display the real images of the distal femur (Fig. 13) and tarsal bone (Fig. 14) acquired with ST and HR imaging plates under the same exposure conditions. In the two figures, the left column illustrates the original images; while on the right are the magnified images of the white rectangles indicated in the original images. It is seen from the magnified images (Fig. 13) that the patellofemoral joint (with a white circle) obtained with the HR plate shows better resolution as compared to ST plate. Similarly, the magnified images of Fig. 14 (the cuneiform and navicular regions indicated by a white arrow) obtained with HR plate shows better resolution as compared to ST plate. The experimental validation provides confirming evidence for the MTF results presented in Fig. 11. As regarding image noise, it can be seen from the magnified images of Figs. 13 and 14 that the images acquired with HR

plates show higher noise levels. The perceptual results correctly reflect the outcome of the NPS shown in Fig. 12.

5. CONCLUSIONS

In this study, we have presented a method for measuring physical performance of medical imaging systems. In this method, mutual information was used to measure combined properties of image noise and resolution of an imaging system. To validate the proposed method, computer simulations were first performed to investigate the effects of noise and resolution degradation on mutual information. Then experiments were conducted to measure the physical performance of an imaging plate in terms of the proposed metric. Our simulation and experimental results confirmed that the combined effect of deteriorated blur and noise on the images can be measured and analyzed using the mutual-information metric. The method is expected to be useful for measuring overall image quality of medical imaging systems.

REFERENCES

- [1] H. Fujita, K. Doi and M.L. Giger, "Investigation of basic imaging properties in digital radiography. 6. MTFs of II-TV digital imaging systems", *Med. Phys.*, vol. 12, pp. 713-720, 1985.
- [2] M. L. Giger, K. Doi and H. Fujita, "Investigation of basic imaging properties in digital radiography. 7. Noise Wiener spectra of II-TV digital imaging systems", *Med. Phys.*, vol. 13, 131-138, 1986.
- [3] C. E. Shannon, "Mathematical theory of communication", *Bell. Syst. Tech. J.*, vol. 27, pp. 379-423, 623-656, 1948.
- [4] C. E. Shannon and W. Weaver, *The Mathematical Theory of Communication*, The University of Illinois Press, Urbana, 1949.
- [5] D. Skerl, B. Likar and F. Pernus, "A protocol for evaluation of similarity measures for rigid registration", *IEEE Trans. Med. Imag.* vol. 25, pp. 779-791, 2006.
- [6] J. P. W. Pluim, J. B. A. Maintz, and M. A. Viergever, "Mutual-information-based registration of medical images: A survey", *IEEE Trans. Med. Imag.* vol. 22, pp. 986-1004, 2003.
- [7] G. D. Tourassi, B. Harrawood, S. Singh and J. Y. Lo, "Information-theoretic CAD system in mammography: Entropy-based indexing for computational efficiency and robust performance", *Med. Phys.*, vol. 34, pp. 3193-3204, 2007.
- [8] Y. Lee, D. Y. Tsai and E. Matsuyama, "A simulation study of radiographic image quality measurement based on transmitted information", *Jpn. J. Radiol. Technol.*, vol. 63, pp. 341-344, 2007.
- [9] D. Y. Tsai, Y. Lee and E. Matsuyama, "Information-entropy measure for evaluation of image", *J. Digit. Imaging*, vol. 21, pp. 338-347, 2008.
- [10] T. M. Cover and J. A. Thomas, *Elements of Information Theory*, Wiley-Interscience, New York, pp. 13-37, 1991.
- [11] F. Attneave, *Applications of Information Theory to Psychology*, Holt, Rinehart and Winston, New York, 1967.
- [12] P. Jr. Sprawls, *Physical Principles of Medical Imaging*, Medical Physics Publishing, Wisconsin, 1995.